SUPPLEMENTARY MATERIALS AND METHODS

Patient data

This study was approved by the institutional review board of the Pasteur Institute of Iran, and all subjects and parents of underaged patients gave written informed consent to participate in research and to publish their images. In this study, 92 extended families affected by nonsyndromic and syndromic forms of ichthyosis, diagnosed in various medical centers in Iran, were evaluated. The families were personally examined by a dermatologist (HM) and by medical geneticists (LY, AK and HV), who are authors, and the diagnostic clinical features and demographic data were carefully recorded. Criteria for inclusion were clinical presentation of ichthyosis supported in some of the patients by histopathology.

Histopathology and Immunofluorescence

Skin biopsies were obtained from a lesional area together with adjacent normal appearing skin of the proband and processed for histopathology with standard techniques. Paraffin sections (5 μm) were stained with Hematoxylin and Eosin. Parallel sections (3 μm) were stained with mouse anti-human connexin 26 antibody (Cx-12H10(13-1800), Life Technologies, Carlsbad, CA), followed by a fluorescein conjugated goat anti-mouse secondary antibody (IRDye 800CW, LI-COR Biosciences, Lincoln, NE). The images were visualized by EVOSTM Auto Imaging System, (Thermo Fisher Scientific, Waltham, MA).

Variant interpretation

SNVs and CNVs were examined using the annotated CSV files of WES from the three affected family members, IV-1, IV-10, and IV-11. The sequence variants were filtered from the VCF files for missense, nonsense, and splice site-affecting variants. Indel variants were

filtered for exonic in-frame insertions and deletions, frameshift mutations, and gained or lost start or stop codon. Additionally, only variants with 1000 Genomes database total frequencies of <0.05 (see Figure 2a), or those without frequency data available, were examined. Candidate genes using these filtering parameters were then overlapped between the three affected individuals in the family to examine potential common disease-causing variants. Considering the given phenotype and segregation analysis allowed us to identify two pathogenic variants in GJB2.

Western blotting: Oocytes extracts were prepared as previously described30, separated on 12% SDS gels and transferred to nitrocellulose membranes. Blots were blocked with 5% milk and 0.1% Tween20 in TBS, probed with polyclonal antibodies against Cx26 (Life Technologies, Carlsbad CA), followed by horseradish peroxidase conjugated secondary antibodies (Jackson Laboratories and GE Healthcare). A monoclonal β-actin antibody (Abcam, Cambridge, MA) was used as a loading control.

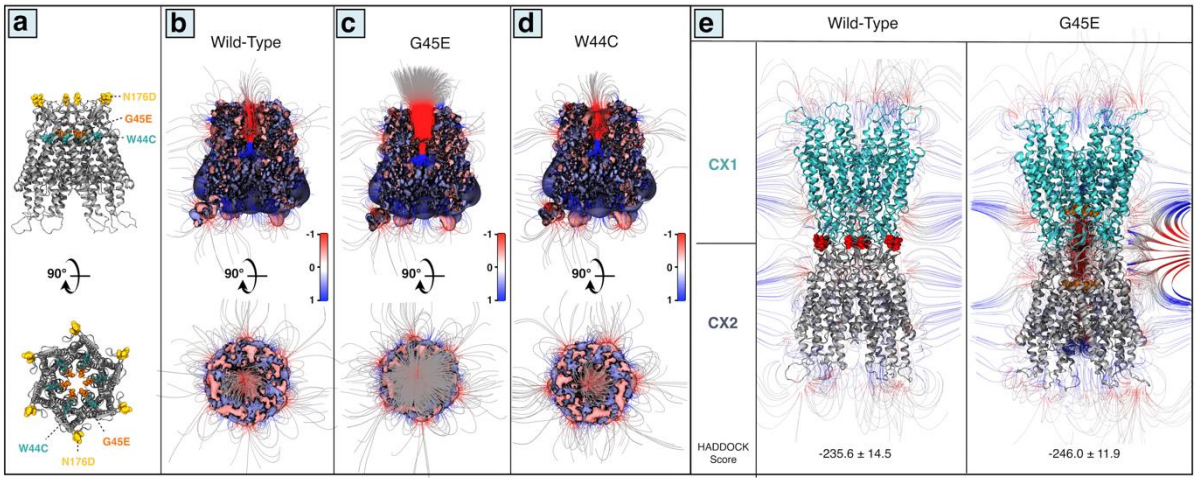

SUPPLEMENTARY FIGURE LEGEND

Supp. Figure S1. Conformations of the mutant Cx26 in hemichannel and channel form. (a) The location of p.Asn176Asp, previously identified in cases with syndromic (p.Gly45Glu) and non-syndromic deafness (p.Trp44Cys) are shown by ribbon representation in yellow, orange and cyan, respectively. (b-d) Electrostatic potential and electrostatic filed-lines of mutants and wild-type are depicted in top- and side-view. Positive and negative potentials are shown in blue and red, respectively (color scale is -1 to +1 kTe^{-1}). (e) The modeled conformation of Cx26 channel in wild-type (left-panel) and p.Gly45Glu (right-panel) by HADDOCK are shown with their electrostatic field-lines. Positive and negative electrostatic potentials are shown in blue and red, respectively (right panel) (color scale is -1 to +1 kTe^{-1}). Note the marked differences in the electrostatic potentials in p.Gly45Glu as compared to p.Asn176Asp mutant, as shown in Figure 4.

<u>Supp. Table S1.</u> Scores and energetic parameters obtained in protein docking of channel conformations of Cx26 by HADDOCK. HADDOCK score represents the best representation of the docking complex based on the weighted sum of contributed energies. WT: wild-type, N176D and G45E mutants.

Type	Complex ID	HADDOCK score	Van der Waals energy (kcal mol^{-1})	Electrostatic energy (kcal mol^{-1})	Desolvation energy (kcal mol^{-1})	Restraint violation energy (kcal mol^{-1})	Buried surface area (Å^2)
WT	1	-235.6 ± 14.5	-328.4 ± 17.8	-502.9 ± 28.3	69.6 ± 9.9	1238.2 ± 94.79	1238.2 ± 94.79
	2	-226.6 ± 19.1	-314.1 ± 5.0	-491.6 ± 22.6	74.0 ± 5.0	1117.8 ± 130.00	6934.7 ± 172.1
	3	-108.6 ± 14.7	-257.0 ± 9.2	-418.8 ± 35.9	95.5 ± 14.6	1366.3 ± 62.55	6396.0 ± 156.7
	4	-103.4 ± 32.3	-245.2 ± 16.7	-405.4 ± 61.0	86.3 ± 13.6	1365.4 ± 206.55	6438.3 ± 193.1
	5	-50.6 ± 58.7	-213.6 ± 51.1	-332.7 ± 109.8	93.2 ± 46.8	1362.7 ± 87.37	6145.5 ± 412.7
N176D	1	-199.5 ± 21.1	-266.0 ± 17.0	-682.6 ± 37.8	65.2 ± 18.5	1378.5 ± 112.84	6459.2 ± 49.0
	2	-138.0 ± 22.5	-190.6 ± 4.8	-599.4 ± 115.6	19.3 ± 45.6	1531.6 ± 71.12	6144.9 ± 153.0
	3	-110.2 ±12.6	-181.2 ±5.5	-548.6 ±67.4	29.9 ±14.7	1508.3 ± 49.32	6027.5 ±57.9
	4	-93.8 ±9.8	-165.3 ±15.4	-495.6 ±59.4	13.2 ±14.5	1574.6 ± 38.76	5937.6 ±104.1
	5	17.8 ±17.8	-120.1 ±21.2	-283.9 ±51.5	24.8 ±3.8	1699.0 ±113.35	4350.8 ±175.0
G45E	1	-246.0 ± 11.9	-312.2 ± 14.9	-444.1 ± 19.5	34.6 ± 10.6	1204.6 ± 163.31	6856.8 ± 186.1
	2	-210.8 ± 13.8	-290.5 ± 13.4	-470.3 ± 39.5	50.9 ± 27.8	1229.0 ± 173.63	6886.7 ± 85.4
	3	-201.2 ± 12.8	-300.7 ± 25.6	-468.8 ± 10.6	55.5 ± 17.2	1377.1 ± 65.63	6991.6 ± 292.6
	4	-174.6 ± 3.8	-297.1 ± 10.9	-431.1 ± 43.1	64.1 ± 12.0	1445.9 ± 61.22	6621.9 ± 101.8
	5	-32.4 ± 17.7	-161.6 ± 11.4	-149.4 ± 18.7	16.2 ± 9.7	1428.9 ± 113.15	5623.8 ± 139.1

<u>Supp. Table S2.</u> Intermolecular hydrogen bonds via ASN176 and ASP176 in modeled channel conformations of Cx26 in wild type and mutant (N176D), respectively with the following measurement criteria: Donor-Acceptor distance: 3.5 Å; Angle cutoff: 30°.

Type	Donor	Chain ID	Donor location	Acceptor	Chain ID	Acceptor location
	LYS168	SegF'	Side	ASN176	SegE	Side
	THR177	SegA'	Side	ASN176	SegA'	Main
	LYS168	SegC	Side	ASN176	SegB'	Side
	LYS168	SegA	Side	ASN176	SegD'	Side
	LYS168	SegC'	Side	ASN176	SegB	Side
WT	ASN176	SegF	Side	ASP179	SegE'	Side
	ASN176	SegD	Side	THR177	SegA'	Main
	ASN176	SegE'	Side	ASP179	SegF	Side
	ASN176	SegD'	Side	ASP179	SegA	Side
	ASN176	SegB	Side	ASP179	SegC'	Side
	ASN176	SegC'	Side	THR177	SegB	Main
	LYS168	SegE'	Side	ASP176	SegF	Side
	LYS168	SegE	Side	ASP176	SegF'	Side
	LYS168	SegF	Side	ASP176	SegE'	Side
	LYS168	SegF'	Side	ASP176	SegE	Side
N176D	LYS168	SegD'	Side	ASP176	SegA	Side
	LYS168	SegD	Side	ASP176	SegA'	Side
	THR177	SegA	Side	ASP176	SegD'	Side
	LYS168	SegA	Side	ASP176	SegD'	Side
	LYS168	SegA'	Side	ASP176	SegD	Side